

Influence of correlations on transitive electron-phonon couplings in cuprate superconductors

G. Seibold,¹ M. Grilli,² and J. Lorenzana³

¹*Institut für Physik, BTU Cottbus, PBox 101344, 03013 Cottbus, Germany*

²*Dipartimento di Fisica, Università di Roma “La Sapienza”, P.le Aldo Moro 5, I-00185 Roma, Italy*

³*ISC-CNR and Dipartimento di Fisica, Università di Roma “La Sapienza”, P.le Aldo Moro 5, I-00185 Roma, Italy*

(Dated: November 12, 2018)

We investigate a model for the CuO₂ plane of high-T_c superconductors where the charge carriers are coupled to A_{1g} and B_{1g} symmetric out-of plane vibrations of the oxygen atoms in the presence of local Hubbard correlations. The coupling is implemented via a modulation of the hopping integral and we calculate the renormalization of vertex and pairing scattering functions based on the time-dependent Gutzwiller approximation. Contrary to local electron-phonon couplings we find that the transitive coupling can even be enhanced by correlations for certain momenta and symmetries of the vibrations. While this effect may be important for certain properties, we find that, with regard to superconductivity, electron-electron correlations still generically lead to a suppression of the pairing correlations. Our results allow for an estimate of correlation effects on the electron-phonon induced pair scattering from weak electron-electron interactions up to the Mott regime. For onsite repulsions relevant to cuprate superconductors our calculations reveal a significant contribution of B_{1g} phonons to d-wave superconductivity.

PACS numbers: 71.27.+a, 74.20.-z, 74.25.Kc, 74.72.-h

I. INTRODUCTION

The search for the new superconducting cuprates by Bednorz and Müller¹ was inspired by the idea that in systems containing Jahn-Teller (JT) ions the strong interaction of electrons with local distortions may lead to high transition temperatures. While meanwhile the contribution of a JT mechanism to superconductivity is controversial, the coupling of electrons to the lattice in cuprates is evidenced in numerous experiments. These include among others the observation of an isotope effect in scanning tunneling microscopy (STM) data² and in T_c away from optimal doping,³ the softening of certain phonons under doping,⁴⁻⁷ and the existence of a critical CuO₄ octahedra tilt angle for the existence of superconductivity in lanthanum cuprates.⁸ Also the kink in the electronic dispersion as seen in angle-resolved photoemission spectroscopy (ARPES) experiments has been attributed to strong electron-phonon (el-ph) interactions⁹ which in Bi₂Sr₂CaCu₂O_{8+δ} compounds is supported by the observation of an isotope effect in the corresponding energy scale¹⁰ (cf. also Ref. 11 and references therein). However, density functional theory (DFT) usually yields an electron-phonon coupling constant which is too small in order to explain the high transition temperatures of the cuprate materials.¹² This becomes even worse when the effect of electronic correlations is considered which are underestimated within the DFT method. Basically, correlations suppress the charge fluctuations and thus the scattering of electrons from phonons, which leads to a further reduction of the el-ph interaction (for a review cf. Refs. 13,14).

In terms of Hubbard type models the el-ph interaction is usually investigated for couplings which arise from an expansion of on-site energies in terms of some vibrational

coordinates^{13,15-17} so that in general both interactions, electronic and electron-phonon, are local or at least have a dominant local contribution.

The interplay of el-el and el-ph interactions leads to a screening of the latter over the whole Brillouin zone which is most pronounced at large momenta.^{15,18} For sizeable correlations the maximum in the phonon self-energy is then shifted from the Peierls wave-vector to $q = 0$, which for strong electron lattice couplings eventually induces a phase separation instability.

Within a slave-boson technique the influence of correlations onto the el-ph interaction has also been investigated within a three-band model where the phonons have been coupled locally to the copper and oxygen density.¹⁹ It was found that generically the renormalization of the el-ph vertex depends on $v_F q / \omega$ (v_F is the Fermi velocity). It turns out to be strongly suppressed if this ratio is $\gg 1$, i.e. in the static limit, while it is almost unaffected in the dynamical limit.

While the interplay between correlations and local (Holstein-type) el-ph interaction is quite well understood, the situation for transitive couplings is less clear. In a lattice model this type of coupling arises from the modulation of hopping integrals due to lattice vibrations. Vertex renormalization effects have been studied in the context of a tJ-model in Ref. 20 and for the $U \rightarrow \infty$ Hubbard model within a slave-boson scheme in Refs. 21,22. We are not aware of any similar investigation for transitive couplings within an approach, which can cover the parameter space from weak coupling up to the Mott regime, which is the task we want to accomplish in the present paper.

In cuprates, transitive electron-phonon couplings are believed to be of significance for the so-called breathing and buckling modes which correspond to in- and out-of

plane motions of the oxygen atoms and which contribute most to the pairing interaction arising from phonons.^{23,24} For example, the inclusion of a screened Coulomb interaction within the LDA-U method²⁵ greatly enhances the el-ph interaction of the half-breathing mode whereas the influence on the full-breathing mode is much weaker. An extensive analysis of the strength and material dependencies of these phonon modes, including also apical oxygen modes, has recently been performed in Ref. 26. It was found that the planar oxygen B_{1g} c-axis modes lead to the strongest enhancement of d-wave superconductivity. Moreover, upon including long-range Coulomb interactions, which in a layered system lead to low energy plasmon excitations Ω_{pl} , the coupling can even be overscreened, i.e. the B_{1g} vertex increases with increasing Ω_{pl} . Again the effect of strong local correlations on the coupling of charge carriers to B_{1g} modes has not been considered in Ref. 26 and is the purpose of the present paper.

Within a one-dimensional model we have previously studied the influence of a transitive el-ph interaction on the phonon self-energy $\Sigma_{ph}(\mathbf{q}, \omega)$.²⁷ Most interestingly it was found that $\Sigma_{ph}(\mathbf{q}, \omega)$ can be enhanced for small momenta upon switching on the Hubbard interaction whereas for large momentum $\Sigma_{ph}(\mathbf{q}, \omega)$ becomes suppressed with U similar to the case of a local (Holstein) el-ph interaction.

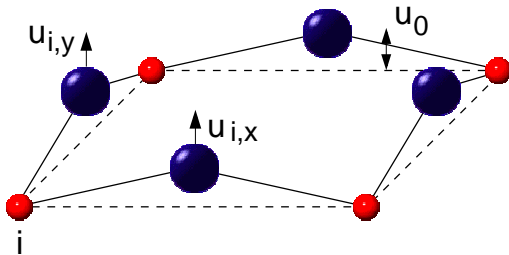


FIG. 1: (Color online) Geometry of the buckled CuO_2 plane with Cu (small, red) and oxygen (large, blue) ions. Electronic degrees of freedom are on the Cu sites and vibrational degrees on the oxygen sites. Notice that the configuration where oxygens on the x-bonds are distorted in the negative z-direction leads to the same model hamiltonian as Eq. (1).

Motivated by this finding we investigate in the present paper the interplay between electronic correlations and a transitive el-ph interaction with regard to the Cooper scattering amplitude. We exemplify this interplay for the buckling mode where electrons couple to out-of-plane (z-direction) motions of the oxygen atoms. For a planar CuO_2 system, due to symmetry, this kind of coupling would be quadratic in the z-coordinates.²⁸ However, for vibrations around static z_0 -displacements of the oxygen atoms one recovers a linear el-ph interaction.

The static configuration of a frozen-in $\mathbf{Q} = (0, 0)$ mode where all oxygen atoms are displaced along the same direction (cf. Fig. 1) corresponds to the buckling of the plane in $\text{YBa}_2\text{Cu}_3\text{O}_7$ (YBCO) and $\text{Bi}_2\text{Sr}_2\text{CaCu}_2\text{O}_8$

(Bi2212) whereas the static $\mathbf{Q} = (\pi, \pi)$ deformation has its realization in the tilting of the CuO_4 octahedra in the low-temperature orthorhombic phase of $\text{La}_{2-x}\text{Sr}_x\text{CuO}_4$ (LSCO). Fig. 1 shows the direction of positive oxygen displacements $\mathbf{u}_{i,x(y)}$ on top of the static deformation. The model which we introduce in the next section is valid for both cases, $\mathbf{Q} = (0, 0)$ and $\mathbf{Q} = (\pi, \pi)$. However, for the latter distortion one has to take into account a staggered positive direction of $\mathbf{u}_{ix(y)}$. Therefore our investigations hold for a broad class of cuprate materials.

For the sake of clarity it should be stated that the interplay between correlations and el-ph interactions strongly depends on the model under consideration. For example, a coupling to local density fluctuations in the three-band model for cuprate superconductors may transform into a transitive coupling when one derives an effective low-energy one-band model by eliminating the high energy degrees of freedom (cf. e.g. Ref. 29). In our paper we are concerned with a one-band hamiltonian with transitive electron-phonon interactions which can be contrasted with analogous calculations for a local Holstein-type coupling in Ref. 18. Nevertheless one should keep in mind that our results may also mimic the local el-ph coupling in related multiband models.

Our paper is organized as follows. In Sec. II we outline the formalism of our calculation which is based on the time-dependent Gutzwiller approximation. Sec. III presents the results of the renormalization of the transitive EPI due to correlation effects and we conclude our investigations in Sec. IV. In both Sec. II and Sec. III we additionally discuss a one-dimensional model for illustrative purposes.

II. FORMALISM

We use an effective one-band hamiltonian where the hopping between neighboring sites is modulated by the displacement of adjacent oxygen atoms from their distorted equilibrium position.³⁰ The geometry of the distorted CuO_2 plane is sketched in Fig. 1. Similar models have been investigated in Refs. 31,32.

The hamiltonian reads

$$H = \sum_{ij\sigma} t_{ij} c_{i\sigma}^\dagger c_{j\sigma} + U \sum n_{i,\uparrow} n_{i,\downarrow} \quad (1)$$

$$+ g_{tr} \sum_{i\sigma,\alpha} u_{i,\alpha} (c_{i\sigma}^\dagger c_{i+\alpha,\sigma} + h.c.) + \sum_{i,\alpha} \left[\frac{p_{i\alpha}^2}{2M} + \frac{1}{2} \omega_0^2 u_{i,\alpha}^2 \right]$$

Here $c_{i\sigma}^{(\dagger)}$ creates (annihilates) an electron on a square lattice and the vibrational degrees of freedom are sitting on the bonds. The parameter t_{ij} is the hopping amplitude between sites i and j . U denotes the local Hubbard repulsion and $u_{i,\alpha}$ with $\alpha = x, y$ is the displacement from equilibrium of the (oxygen) atom at position $i + \alpha/2$ (cf. Fig. 1). g_{tr} is the coupling parameter between lattice displacement and electronic nearest-neighbor hopping. The

last term in Eq. (1) corresponds to kinetic and elastic energy of the oxygens.

Our approach is based on the time-dependent Gutzwiller approximation (TDGA)³⁴ which gives an accurate description of charge fluctuations of the Hubbard model^{34,35} and which previously has been successfully applied to the study of vertex renormalizations in the Hubbard-Holstein model.¹⁸ The idea is to evaluate the energy of Eq. (1) in the presence of an arbitrary lattice distortion and charge fluctuation within the Gutzwiller approximation (GA)⁴³⁻⁴⁵ and to expand the functional up to second order in the lattice Q_q^\pm and electronic density fluctuations.

The Gutzwiller variational wave function has the form $|\Psi_g\rangle = P_g|SD\rangle$ where P_g is the Gutzwiller projector and $|SD\rangle$ a Slater determinant. For $|SD\rangle$ we use a state with an arbitrary charge profile. We define the associated one-body density as $\rho_{ij\sigma} = \langle SD|\hat{c}_{j\sigma}^\dagger \hat{c}_{i\sigma}|SD\rangle$. Since magnetic and charge excitations decouple we can restrict to Slater determinants with $\rho_{ij\uparrow} = \rho_{ij\downarrow}$.

Our expansion below will be in terms of the density fluctuations of the SD which physically describes quasiparticles and not physical electrons.⁴⁶ The two densities coincide in the onsite case $\rho_{ii\sigma}$ while for off-diagonal density the real particle densities are given by $z_{i\sigma} z_{j\sigma} \rho_{ij\sigma}$ where $z_{i\sigma}$ denote the Gutzwiller renormalization factors.

The quasiparticle density fluctuations that enter into the problem are

$$\begin{aligned} \delta \mathbf{X}_{\mathbf{q}} &= \sum_{k,\sigma} \mathbf{V}(\mathbf{k}, \mathbf{q}) \delta \rho_{k+\mathbf{q},k,\sigma} \\ &= \sum_{k,\sigma} \begin{pmatrix} 1 \\ \epsilon^0(\mathbf{k}) + \epsilon^0(\mathbf{k} + \mathbf{q}) \\ 2 \cos(k_x + \frac{q_x}{2}) \\ 2 \cos(k_y + \frac{q_y}{2}) \end{pmatrix} \delta \rho_{k+\mathbf{q},k,\sigma} \end{aligned} \quad (2)$$

with $\epsilon^0(\mathbf{k})$ being the Fourier transformed of the hopping t_{ij} . In the vector Eq. (2) the first two components δX_q^1 and δX_q^2 correspond to local and transitive density fluctuations, the latter being generated in the expansion of the kinetic energy. The δX_q^3 and δX_q^4 components are also transitive fluctuations but arise from the expansion of the el-ph coupling.

The expansion results in

$$\delta E^{GA} = E_{ee}^{(2)} + E_{coup}^{(2)} + E_{ph}^{(2)}. \quad (3)$$

where the first term describes the interaction between electronic density fluctuations

$$E_{ee}^{(2)} = \frac{1}{2N} \sum_{\mathbf{q}} \begin{pmatrix} \delta X_{\mathbf{q}}^1 \\ \delta X_{\mathbf{q}}^2 \end{pmatrix} \underline{W}_{\mathbf{q}}^{ee} \begin{pmatrix} \delta X_{-\mathbf{q}}^1 \\ \delta X_{-\mathbf{q}}^2 \end{pmatrix} \quad (4)$$

and the elements of the interaction kernel

$$\underline{W}_{\mathbf{q}}^{ee} = \begin{pmatrix} A_{\mathbf{q}} & B_{\mathbf{q}} \\ B_{\mathbf{q}} & C_{\mathbf{q}} \end{pmatrix} \quad (5)$$

are defined in the appendix.

The interaction between electronic density and lattice fluctuations $Q_q^\alpha = 1/\sqrt{N} \sum_i \exp[-i\mathbf{q}\mathbf{R}_{i+\alpha/2}] u_{i,\alpha}$ is described by the second term

$$E_{coup}^{(2)} = \frac{1}{\sqrt{N}} \sum_{q,i,\alpha=x,y} \gamma_q^{i,\alpha} \delta X_q^i Q_{-q}^\alpha \quad (6)$$

with

$$\gamma_q^{1,\alpha} = 2g_{tr} K B_q \cos(\frac{q_\alpha}{2}) \quad (7)$$

$$\gamma_q^{2,\alpha} = 2g_{tr} K C_q \cos(\frac{q_\alpha}{2}) \quad (8)$$

$$\gamma_q^{3,\alpha} = g_{tr} z_0^2 \delta_{\alpha,x} \quad (9)$$

$$\gamma_q^{4,\alpha} = g_{tr} z_0^2 \delta_{\alpha,y} \quad (10)$$

and $K \equiv \frac{2}{N} \sum_{k,\sigma} \cos(k_x) \langle n_{k,\sigma} \rangle$. z_0 denotes the hopping renormalization factor in the GA which generically decreases with U and at half-filling vanishes at the Brinkmann-Rice transition U_{BR} .³³

In the derivation of Eqs. (4)-(6) [and the following Eq. (11)] we have already 'adiabatically' eliminated^{18,27,34,35} the double occupancy fluctuations which arise in the expansion of the GA functional within the TDGA prescription. For the present model the corresponding formal procedure is analogous to that described in Ref. 27.

Notice that on the GA level the coupling to the lattice fluctuations is reduced $\sim z_0^2$ by the correlations. However, the TDGA induces additional couplings to local ($\delta X_{\mathbf{q}}^1$) and transitive ($\delta X_{\mathbf{q}}^2$) density fluctuations and we will show below that in certain cases this will even lead to an enhancement of the electron-phonon vertex.

Finally we obtain for the lattice energy

$$E_{ph}^{(2)} = \frac{1}{2N} \sum_{q,\alpha\beta} M (\Omega_q^{\alpha\beta})^2 Q_q^\alpha Q_{-q}^\beta \quad (11)$$

and it turns out that the elimination of the double occupancy introduces a novel renormalization and a mixing of the x, y -buckling modes:

$$(\Omega_q^{\alpha\beta})^2 = \omega_0^2 \delta_{\alpha\beta} - \kappa_q^2 \cos(\frac{q_\alpha}{2}) \cos(\frac{q_\beta}{2}) \quad (12)$$

$$\kappa_q^2 = -\frac{1}{M} (2g_{tr})^2 K_\alpha K_\beta C_q. \quad (13)$$

The eigenmodes are obtained from the transformation

$$\begin{pmatrix} Q_q^x \\ Q_q^y \end{pmatrix} = \underline{U} \begin{pmatrix} V_q^{B1g} \\ V_q^{A1g} \end{pmatrix} \quad (14)$$

with

$$\underline{U} = \frac{1}{\sqrt{\cos^2(\frac{q_x}{2}) + \cos^2(\frac{q_y}{2})}} \begin{pmatrix} \cos(\frac{q_y}{2}) & \cos(\frac{q_x}{2}) \\ -\cos(\frac{q_x}{2}) & \cos(\frac{q_y}{2}) \end{pmatrix}$$

and correspond to out- (i.e. B_{1g} symmetry) and in- (i.e. A_{1g} symmetry) phase oscillations of the x/y oxygen atoms.

The eigenfrequencies read as

$$\begin{aligned}\omega_q^{B_{1g}} &= \omega_0 \\ \omega_q^{A_{1g}} &= \sqrt{\omega_0^2 - \kappa_q^2 (\cos^2(\frac{qx}{2}) + \cos^2(\frac{qy}{2}))}.\end{aligned}$$

Thus the frequency of the A_{1g} mode softens due to the elimination of the double occupancy fluctuations as a natural consequence of the interaction between both bosonic degrees of freedom. There will be an additional softening due to phonon self-energy effects. In the following we plot results in dependence of the coupling parameter $\lambda = g_{tr}^2/\omega_0$ using the *bare* phonon frequencies. One should therefore keep in mind that the inclusion of the correlation induced phonon softening would give an additional (small) enhancement in the A_{1g} channel.

In order to compute vertex corrections and the effective interaction between quasiparticles we introduce correlation functions χ_q^{ij} which describe the response of the quasiparticle (Slater determinant) density fluctuations δX_q^i [Eq. (2)] to an external perturbation $\delta \lambda_q^i$

$$X_q^i = \chi_q^{ij} \lambda_q^j.$$

It is convenient to represent the non-interacting susceptibilities as

$$\underline{\underline{\chi}}_q^0(\omega) = \begin{pmatrix} \underline{\underline{\chi}}_q^{ee,0} & \underline{\underline{\chi}}_q^{ex,0} \\ \underline{\underline{\chi}}_q^{xe,0} & \underline{\underline{\chi}}_q^{xx,0} \end{pmatrix}$$

where e.g. the 2×2 susceptibility matrix $\underline{\underline{\chi}}_q^{ee,0}$ corresponds to the submatrix of $\chi_{ij}(\mathbf{q})$ for $i, j = 1, 2$ and the definition of the other block matrices follows analogously. Notice that here and in the following we denote 4×4 (2×2) matrices with a double (single) underscore.

The lattice induced (bare) interaction is obtained by assuming that the phonon frequencies are larger than the frequencies of the electronic excitations of interest. Therefore we can eliminate the lattice eigenmodes for a frozen electronic configuration, $\partial E^{GA}/\partial V_q^s = 0$ ($s = B_{1g}, A_{1g}$). One obtains in addition to Eq. (4) a

lattice induced (bare) interaction between density fluctuations

$$V_{ij}^{ee}(\mathbf{q}) = -\frac{1}{2N} \sum_{q,s,\alpha\beta} \frac{1}{M\omega_q^s} \gamma_q^{i,\alpha} \gamma_{-q}^{j,\beta} U_q^{\alpha,s} U_{-q}^{\beta,s}. \quad (15)$$

Using the TDGA, this interaction together with the bare Hubbard part Eq. (4) can be dressed by the electronic density fluctuations similar to conventional RPA theory. We define the 'undressed' interaction from the sum of Eqs. (5,15)

$$\underline{\underline{V}}^0(\mathbf{q}) = \underline{\underline{V}}^{ee}(\mathbf{q}) + \begin{pmatrix} \underline{\underline{W}}_q^{ee} & \underline{\underline{0}} \\ \underline{\underline{0}} & \underline{\underline{0}} \end{pmatrix} \quad (16)$$

which upon resumming the RPA leads to the effective dressed interaction between quasiparticles

$$\underline{\underline{W}}^{eff}(\mathbf{q}) = \underline{\underline{V}}^0(\mathbf{q}) \left[\mathbf{1} - \underline{\underline{\chi}}_q^0 \underline{\underline{V}}^0(\mathbf{q}) \right]^{-1}. \quad (17)$$

Finally we can use Eq. (17) to define the Cooper pair scattering amplitude

$$\Gamma(\mathbf{k}, \mathbf{q}) = \sum_{i,j} \underline{\underline{W}}_{ij}^{eff}(\mathbf{q}) V_i(\mathbf{k}, \mathbf{q}) V_j(-\mathbf{k}, -\mathbf{q}) \quad (18)$$

and the $V_i(\mathbf{k}, \mathbf{q})$ have been defined in Eq. (2). We will usually take both \mathbf{k} and $\mathbf{k} + \mathbf{q}$ on the Fermi surface and restrict to the static limit ($\omega = 0$).

We can expand Eq. (18) up to order $\sim g_{tr}^2$ in the phonon contribution. The coefficient of $\sim g_{tr}^2$ defines the second order el-ph contribution to the pair scattering amplitude as

$$\Gamma_s^{(2)}(\mathbf{k}, \mathbf{q}) = -\frac{1}{\omega_q^s} \sum_{i,j} \tilde{\gamma}_q^{i,s} \tilde{\gamma}_{-q}^{j,s} V_i(\mathbf{k}, \mathbf{q}) V_j(-\mathbf{k}, -\mathbf{q}). \quad (19)$$

This scattering amplitude does not include the direct scattering amplitude due to el-el interactions. It includes only el-ph interactions which are, however, renormalized by the el-el interactions.

Here the dressed vertex functions are given by

$$\tilde{\gamma}_q^{i,s} = \begin{pmatrix} \left[\mathbf{1} - \underline{\underline{W}}_q^{e-e} \underline{\underline{\chi}}_q^{ee,0} \right]^{-1} \underline{\underline{W}}_q^{e-e} \left[\mathbf{1} - \underline{\underline{\chi}}_q^{ee,0} \underline{\underline{W}}_q^{e-e} \right]^{-1} \underline{\underline{\chi}}_q^{ex,0} \\ 0 \end{pmatrix}_{ij} \gamma_q^{j,\alpha} U_q^{\alpha,s}. \quad (20)$$

From Eqs. (20,19) it turns out that the original coupling between buckling modes and density fluctuations ($\gamma_q^{3,x}, \gamma_q^{4,y}$), Eq. (9), does not get renormalized by the TDGA but it is only reduced via the z_0 factors already present on the GA level. This also implies that within standard (Hartree-Fock based, i.e. $z_0 = 1$) perturbation

theory a transitive el-ph interaction remains unrenormalized up to second order in the coupling constants. On the other hand, the TDGA can even induce an 'antiscreening' of the local and transitive fluctuations, leading to an enhancement of the $\tilde{\gamma}_q^{i,s}$ as compared to the bare couplings $\gamma_q^{i,\alpha}$ (cf. next section).

Illustrative one-dimensional model

In order to better illustrate the influence of correlations on the el-ph interaction within our TDGA approach, we will consider also a simpler one-dimensional model (cf. Fig. 2). The result of this and the two-dimensional system will be presented in Sec. III.

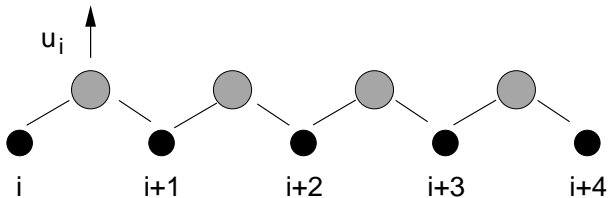


FIG. 2: One-dimensional CuO model where the oxygens (light shaded circles) oscillate perpendicular to the chain. The hopping between nearest-neighbor Cu (full circles) atoms i and $i + 1$ is then linearly expanded in u_i .

The transformation of the previously developed formalism to the one-dimensional model is straightforward. Since there is only one vibrational degree of freedom the relevant fluctuations are

$$\begin{aligned} \delta X_q &= \sum_{k,\sigma} V(k,q) \delta \rho_{k+q,k,\sigma} \\ &= \sum_{k,\sigma} \left(\frac{1}{2 \cos(k+q/2)} \left(\epsilon^0(k) + \epsilon^0(k+q) \right) \right) \delta \rho_{k+q,k,\sigma} \end{aligned} \quad (21)$$

with a dispersion $\epsilon_k^0 = -2t \cos(k)$. For the bare vertices one obtains

$$\gamma_q^1 = 2g_{tr} K B_q \cos(q/2) \quad (22)$$

$$\gamma_q^2 = 2g_{tr} K C_q \cos(q/2) \quad (23)$$

$$\gamma_q^3 = g_{tr} z_0^2 \quad (24)$$

with $K = \frac{4}{\pi} \sin(k_F)$.

III. RESULTS

A. One-dimensional case

Before turning to the two-dimensional cuprate model it is instructive to analyze the model for a linear CuO chain, where the oxygens oscillate perpendicular to the chain direction. Fig. 3 shows the elements of the electronic interaction kernel Eq. (5) for $q = 0$. $A_{q=0}$ corresponds to the interaction between local density fluctuations. Close to half-filling it develops a pronounced maximum at the Brinkmann-Rice transition U_{BR} where it actually diverges at exactly $n = 1$. The coefficient $B_{q=0}$ mixes local and transitive density fluctuations and vanishes at half-filling. However, away from $n = 1$, $|B_q|$

increases upon approaching U_{BR} and also stays finite beyond this value [cf. Fig. 3(b)]. Finally, the coefficient C_q [Fig. 3(c)] corresponds to the interaction between transitive density fluctuations. It also develops a maximum close to U_{BR} , but vanishes in the $U \rightarrow \infty$ limit.

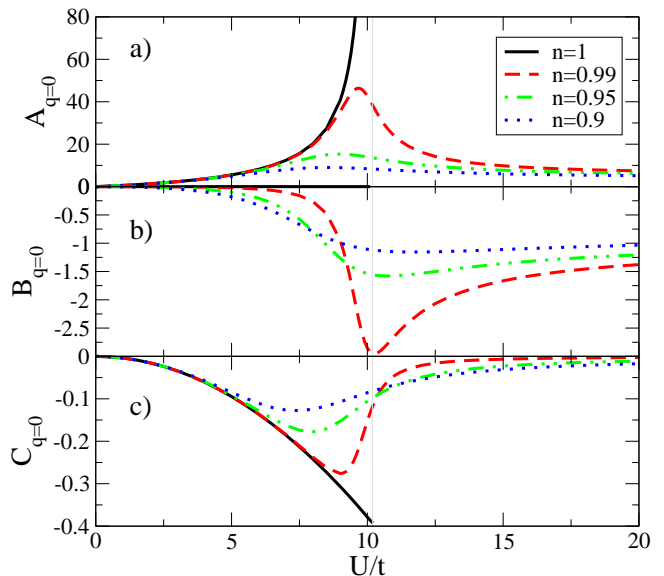


FIG. 3: (Color online) Elements of the electronic interaction kernel Eq. (5) for $q = 0$ as a function of U and different fillings in the one-dimensional CuO model. The vertical line at $U/t = 32/\pi$ corresponds to the Brinkmann-Rice transition.

Let us now turn to the discussion of the renormalized vertex functions via the scattering amplitude $\Gamma^{(2)}/z_0^2$ which is shown in Fig. 4. Notice that we divide by the GA renormalization factor which originates from the density of states renormalization $N^* = N_0/z_0^2$ within the GA. Indeed, upon plotting $\Gamma^{(2)}/z_0^2$ we take into account the interaction in both quantities. We point out that the bare coupling on the GA level is $\sim g_{tr} z_0^2$, which for the 'bare' scattering amplitude would result in a reduction of $\Gamma^0/z_0^2 \sim g_{tr}^2 z_0^2$ upon increasing U/t .

In the one-dimensional model we have just two Fermi points so that the scattering of pairs on the 'Fermi surface' is restricted to $q = 0$ and $q = 2k_F$, respectively. Consider first the $q = 0$ case which is shown in Fig. 4(a). At half-filling the scattering amplitude is identically zero since in this case the chemical potential is at $E_F = 0$ so that the only non-vanishing fluctuations are the local ones [cf. Eq. (21) where for $\mathbf{q} \rightarrow 0$ the fluctuations are restricted to $k = k_F = \pm\pi/2$ and $\epsilon^0(k_F) = 0$]. Although these are coupled to the vibrations via the coefficient B_q [cf. Eq. (22)], this latter also vanishes at $n = 1$, leading to the vanishing of the scattering amplitude. Slightly below half-filling (dashed line in Fig. 4a) one obtains an increase in $\Gamma^{(2)}/z_0^2$ which can be shown to be due to the behavior of the renormalized coupling $\tilde{\gamma}_{q=0}^2 \sim B_{q=0}/(1 + A_{q=0} N^*)$ to the transitive density fluctuations. It is the concomitant increase of $|B_{q=0}|$ around

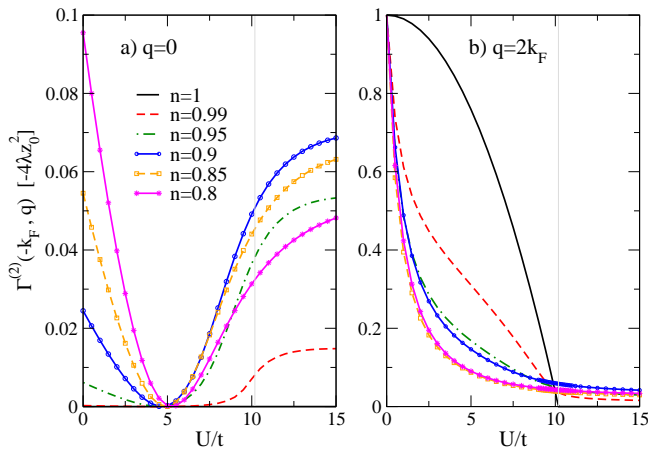


FIG. 4: (Color online) Second order pair scattering amplitude $-\Gamma^{(2)}(\mathbf{k}, \mathbf{q})/(4\lambda z_0^2)$ for the one-dimensional model as a function of U . a) Scattering with $\mathbf{q} = 0$ at $\mathbf{k} = -\mathbf{k}_F$; b) Scattering between $\pm\mathbf{k}_F$ with $\mathbf{q} = 2\mathbf{k}_F$. The vertical line at $U/t = 10.19$ marks the Brinkmann-Rice transition.

U_{BR} together with the reduced screening from local density fluctuations ($\sim 1/(1 + A_{q=0}N^*)$) for $U/t > U_{BR}$, which leads to the peculiar behavior of $\Gamma^{(2)}/z_0^2$ slightly below half-filling and $q = 0$. Remarkably, close to half-filling the scattering amplitude is amplified by large interactions and it becomes many times larger than the scattering amplitude in the non interacting case. This is just the opposite of what happens in the case of Holstein like couplings.

For larger values of the doping the bare coupling $\gamma_{q=0}^3$ dominates the value of $\Gamma^{(2)}/z_0^2$ for small values of U/t which therefore acquires a minimum between $U/t = 0$ and U_{BR}/t .

In the case of $q = 2k_F$ scattering the behavior is simpler. At half-filling ($k_F = \pi/2$) it can be seen from Eqs. (22, 23) that only the bare coupling ($g_{tr}z_0^2$) survives. For $n = 1$ this is not affected by the screening from density fluctuations. The $n = 1$ result in Fig. 4b (solid line) therefore simply reflects the behavior of z_0^2 as a function of U/t and vanishes at $U_{BR} = 32t/\pi$. Away from half-filling the additional screening leads to a further reduction of the scattering amplitude which continuously decreases with increasing U/t even beyond U_{BR} .

B. Two-dimensional model

From the analysis of the 1D model we have learned that within our TDGA analysis, correlations can enhance the vertex for small momentum transfer. On the other hand, correlations generically reduce the coupling for large q scattering. We now investigate whether this result persists for the model in two dimensions, introduced at the beginning of the previous section.

In the following figures we discuss the renormalized vertex function from the second order pair scattering

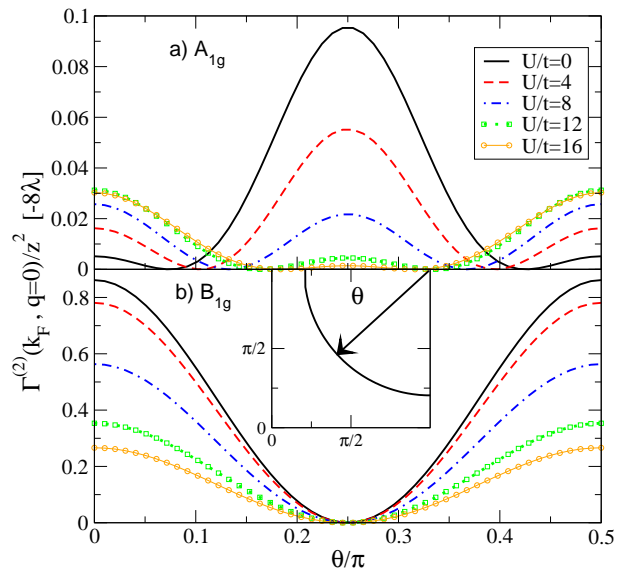


FIG. 5: (Color online) Scattering function $-\Gamma^s(\mathbf{k}_F, \mathbf{q} = 0)/z_0^2$ (in units of 8λ) for various values of U/t and zero momentum transfer of pairs on the Fermi surface. Coupling to A_{1g} (a) and B_{1g} (b) modes. Parameters: $\delta = 0.1$, $t'/t = -0.4$.

amplitude $\Gamma^{(2)}(\mathbf{k}_F, \mathbf{q}_F)/z_0^2$ [cf. Eq. (19)] in units of -8λ which makes this quantity dimensionless and positive. The factor of 'eight' originates from the definition of the bare coupling Eqs. (6, 14) which (for $\mathbf{q} = 0$) is given by $g_{tr}z_0^2\sqrt{2}[\cos(k_x) - \cos(k_y)]$ for B_{1g} - and $g_{tr}z_0^2\sqrt{2}[\cos(k_x) + \cos(k_y)]$ for A_{1g} symmetry so that $8g_{tr}^2/\omega_0 \equiv 8\lambda$ corresponds to the maximum scattering amplitude for $U/t = 0$.

In Fig. 5 we show the second order scattering function Eq. (19) for pairs on the Fermi surface and zero momentum transfer, i.e. $\Gamma^{(2)}(\mathbf{k}_F, \mathbf{q} = 0)$. For A_{1g} -symmetry the coupling function is $\sim \cos(k_x) + \cos(k_y)$ so that the $U = 0$ scattering is largest around the nodes. For a B_{1g} -type coupling $\sim \cos(k_x) - \cos(k_y)$ the $U = 0$ scattering is maximized around the antinodes. This interaction becomes continuously suppressed upon increasing U/t . Remarkably the vertex function from the coupling to A_{1g} modes is instead enhanced around the antinodal regions while it is also suppressed around the nodes. As in the one-dimensional case, the enhancement by the interaction contrasts the corresponding findings for local couplings.

Figs. 6, 7, 8 display $\Gamma^{(2)}(\mathbf{k}, \mathbf{q})/z_0^2$ for a fixed momentum $\mathbf{k} + \mathbf{q}$ of the scattered pair on the FS (cf. inset).

For the scattering from the A_{1g} -type mode the generic trend is a correlation induced enhancement of the vertex function when the pairs are scattered between the antinodal regions. In all other cases correlations generically suppress the scattering from the A_{1g} mode. Since the enhancement occurs only for those regions in momentum space $\mathbf{k} \approx \mathbf{k}_{antinodes}$ where the vertex is small, the overall effect is thus a suppression of the coupling upon increasing U/t .

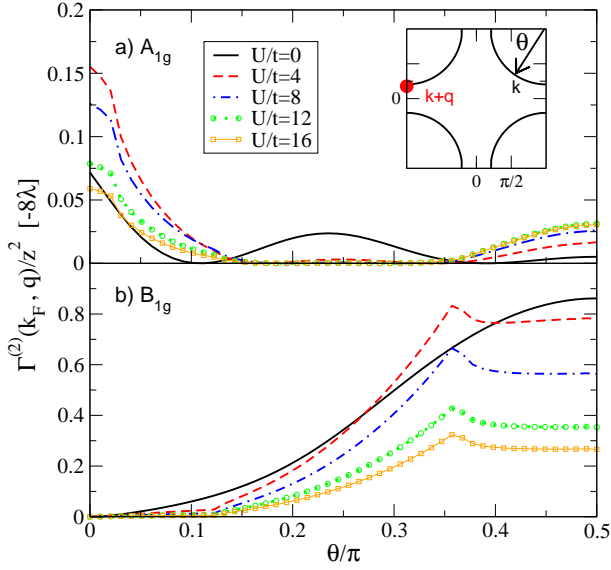


FIG. 6: (Color online) Scattering function $-\Gamma^{(2)}(\mathbf{k}_F, \mathbf{q})$ for pairs on the Fermi surface as indicated in the inset. Coupling to A_{1g} (a) and B_{1g} (b) modes. Dressed (solid) and bare (dashed) vertex along selected symmetry directions in the Brillouin zone. $\delta = 0.1$, $t'/t = -0.4$.

In the case of scattering from the B_{1g} mode, one observes a suppression for all momenta \mathbf{k} and $\mathbf{k} + \mathbf{q}$. In fact, as in the one-dimensional case a correlation induced enhancement of the vertex is due to the coupling to transitive density fluctuations (i.e. δX_q^2). It turns out that this coupling vanishes for B_{1g} symmetry leading to a generic suppression of the coupling in contrast to the A_{1g} mode.

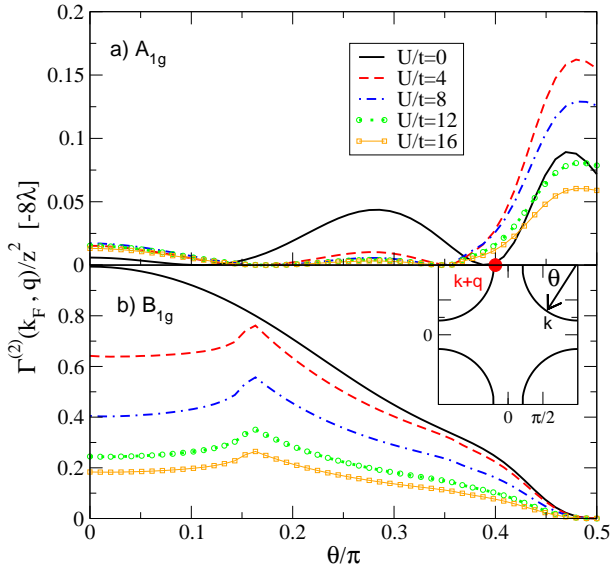


FIG. 7: (Color online) Scattering function $-\Gamma^{(2)}(\mathbf{k}_F, \mathbf{q})$ for pairs on the Fermi surface as indicated in the inset. Coupling to A_{1g} (a) and B_{1g} (b) modes. Dressed (solid) and bare (dashed) vertex along selected symmetry directions in the Brillouin zone. $\delta = 0.1$, $t'/t = -0.4$.

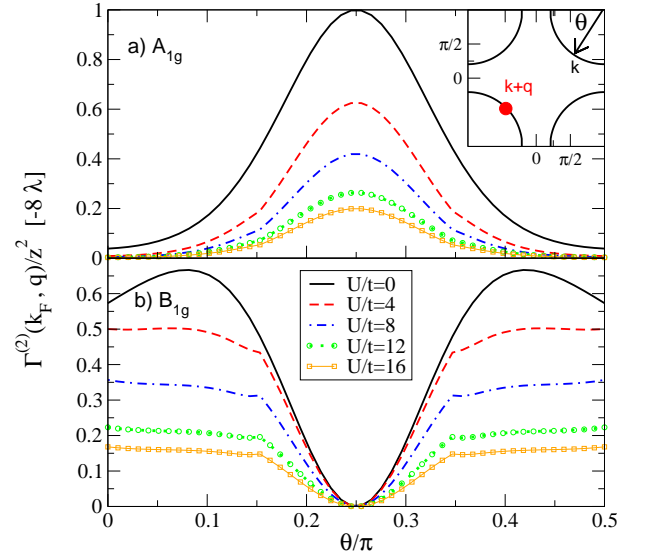


FIG. 8: (Color online) Scattering function $-\Gamma^s(\mathbf{k}_F, \mathbf{q})$ for pairs on the Fermi surface as indicated in the inset. Coupling to A_{1g} (a) and B_{1g} (b) modes. Dressed (solid) and bare (dashed) vertex along selected symmetry directions in the Brillouin zone. $\delta = 0.1$, $t'/t = -0.4$.

In order to quantify the influence of correlations on superconductivity we calculate the average of the scattering amplitude over the Fermi surface, weighted by the symmetry function for different gap symmetries. We consider the following function

$$\langle \Gamma \rangle = \frac{\frac{1}{N^2} \sum_{\mathbf{k}\mathbf{p}} \delta(\epsilon_{\mathbf{k}} - E_F) \delta(\epsilon_{\mathbf{p}} - E_F) \gamma_{\mathbf{k}} \gamma_{\mathbf{p}} \Gamma(\mathbf{k}, \mathbf{p} - \mathbf{k})}{\frac{1}{N} \sum_{\mathbf{k}} \delta(\epsilon_{\mathbf{k}} - E_F) (\gamma_{\mathbf{k}})^2} \quad (25)$$

and $\gamma_{\mathbf{k}}$ specifies isotropic s-wave (is), anisotropic s-wave (as) and d-wave (d) symmetry:

$$\gamma_{\mathbf{k}} = \begin{cases} 1 & (\text{is}) \\ (\cos(k_x) + \cos(k_y))/2 & (\text{as}) \\ (\cos(k_x) - \cos(k_y))/2 & (\text{d}). \end{cases}$$

For the scattering amplitude $\Gamma(\mathbf{k}, \mathbf{p} - \mathbf{k})$ we first use the second order expression Eq. (19) in order to study the influence of vertex corrections on SC separately (cf. Fig. 9). Then the fully dressed expression Eq. (18) is used which, besides the repulsive Hubbard interaction Eq. (4) contains all higher order contributions to the screening beyond $\mathcal{O}(g_{tr}^2)$ (cf. Fig. 10).

Fig. 9 displays the average second order el-ph scattering amplitude for different dopings. Notice that a negative sign of $\langle \Gamma \rangle$ signals an attractive interaction whereas a positive value signals the suppression of the corresponding SC order (Ref. 26 uses the opposite convention). The largest coupling is obtained for B_{1g} symmetry where the isotropic s-wave pair scattering is more attractive than that for d-wave pairs since we are analyzing only the renormalized el-ph interaction without the direct effect of the Coulomb repulsion on the scattering amplitude. In

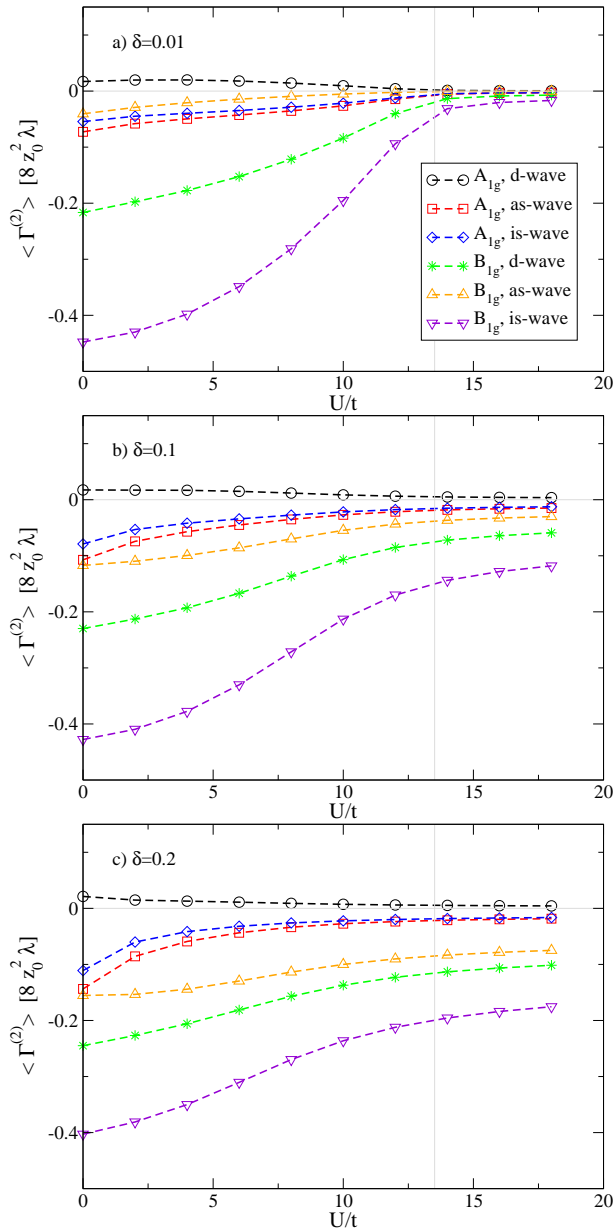


FIG. 9: (Color online) Average of the second order scattering function $\langle \Gamma_s^{(2)}(\mathbf{k}_F, \mathbf{q}) \rangle$ (cf. Eq. (25)) over the Fermi surface weighted with d-wave, anisotropic (as) and isotropic (is) s-wave symmetry functions. $\delta = 0.01$ (upper panel), $\delta = 0.1$ central panel, $\delta = 0.2$ lower panel; $t'/t = -0.4$. The vertical bar in the panels marks the Brinkmann-Rice transition for the half-filled system.

both channels, B_{1g} and A_{1g} , and for all symmetries the average scattering from the modes continuously decreases with increasing U/t due to the reduction of the respective vertices. In the parameter range $U \ll U_{BR}$ it turns out that $\langle \Gamma^{(2)} \rangle$ is not much affected by doping. On the other hand one finds that for U/t beyond the Brinkmann-Rice limit and doping close to half-filling (Fig. 9a) the scattering amplitudes becomes negligibly small but start to increase for finite doping.

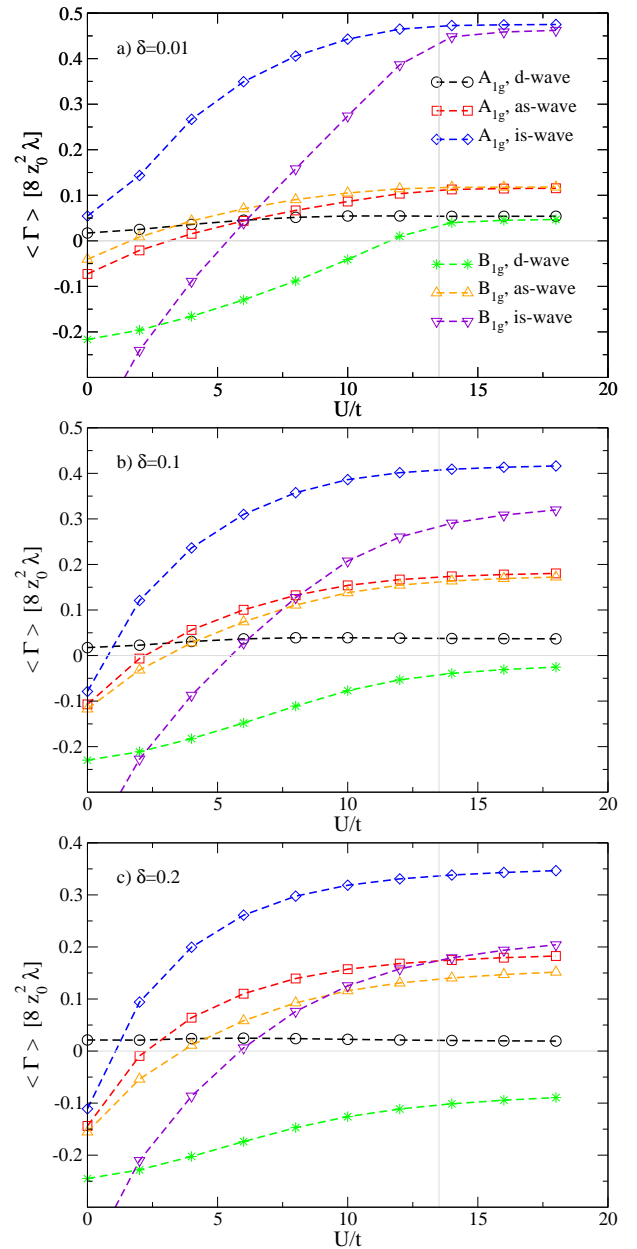


FIG. 10: (Color online) Average of the full scattering function $\langle \Gamma_s(\mathbf{k}_F, \mathbf{q}) \rangle$ (cf. Eq. (25)) over the Fermi surface weighted with d-wave, anisotropic (as) and isotropic (is) s-wave symmetry functions. $\delta = 0.01$ (a), $\delta = 0.1$ (b), and $\delta = 0.2$ (c). $t'/t = -0.4$, $\lambda = g^2/\omega_0 = 0.5$. The vertical line in the panels marks the Brinkmann-Rice transition for the half-filled system.

The average scattering from the A_{1g} symmetric mode is small for both s- and d-wave channels since $\langle \Gamma \rangle$ is only large when the form factor of the SC pairs is small. Therefore as anticipated before the pairs cannot take advantage from the correlation induced enhancement of the vertex in this case. For d-wave symmetry the effective el-el interaction even becomes slightly repulsive. Notice that in the A_{1g} channel the anisotropic s-wave scatter-

ing is slightly larger than that for isotropic s-wave pairs. However, upon analyzing Eq. (25) we find that this effect is due to the normalization (i.e. the denominator), whereas the numerator is larger for isotropic s-wave scattering as it should.

Finally we show in Fig. 10 the result for the full averaged pair scattering amplitude for both d- and s-wave symmetries. The inclusion of the Hubbard derived quasiparticle repulsion Eq. (4) in the interaction part leads to further separation between d- and s-wave symmetries. Since this interaction is almost structureless in momentum space it mainly leads to a suppression of s-wave pair scattering (mostly pronounced for isotropic s-wave) whereas the d-wave pairs are only weakly affected. The latter feel the local Coulomb interaction mainly in the Mott-regime where at half-filling the corresponding scattering now also becomes repulsive. The inclusion of screening processes beyond $\mathcal{O}(g_{tr}^2)$ via the RPA resummation starts to play a role at higher doping where it reduces the strong dependence of $\langle\Gamma\rangle$ on U/t . According to our investigations the attractive scattering of d-wave pairs in the B_{1g} channel dominates for $U/t \gtrsim 2.5$ over the corresponding isotropic s-wave pairing and for $U/t \gtrsim 5.5$ remains the only attractive pairing symmetry within our model.

It should be mentioned that the GA correctly describes band narrowing and the suppression of charge fluctuations but it fails to describe the emergence of the magnetic J scale in the metal as the Mott insulator is approached from the Fermi liquid side. Therefore our present approach does not capture pairing due to the exchange of magnetic fluctuations. Accordingly, if we neglect the el-ph interaction the scattering amplitude becomes repulsive in all the channels considered.

IV. CONCLUSION

The aim of the present paper was to investigate the influence of an on-site electronic repulsion onto a transitive electron-phonon coupling within a single-band Hubbard model. In contrast to similar calculations for a local Holstein-type coupling¹⁸ where the electron-phonon vertex is suppressed for all momenta (but most strongly for large \mathbf{q}), we have seen that a transitive el-ph interactions leads to a much more interesting interplay between electronic correlations and phonons. Our finding that there can even be a correlation-induced enhancement of the pair scattering amplitude for certain momenta is especially important with regard to the anisotropy of the el-ph interaction in cuprate superconductors²⁹. In this regard our approach extends to the correlated regime, the analysis of Refs. 26,29, which were based on a (electronically) non-interacting model.

The correlation-induced enhancement of the electron phonon interaction it is not followed by a similar enhancement of the overall influence of phonons on superconductivity. Even in the present case the impact of phonons

on superconductivity is suppressed by the Coulomb interactions. This is because the enhancement happens in a channel that is not beneficial for d-wave superconductivity, namely A_{1g} , and also because it happens in a restricted momentum range. Notwithstanding the effect on superconductivity, there may be a larger impact on other properties which are more sensitive to the local, rather than the global, momentum dependence like the appearance of kinks on the electron dispersion due to self-energy effects. Also the enhancement of the scattering function at small momentum can play an important role in phase separation instabilities.⁴⁷

We have presented our results as a function of U . A crucial question concerns the strength of electronic correlations in the high- T_c materials. In fact, the early classification of these compounds as doped Mott insulators has recently been questioned in Ref. 36. This point of view agrees with our own estimate for $U/t \approx 8$ as derived from a fitting to the spin-wave dispersion of undoped lanthanum cuprates^{37,38} and which is almost half the value of the Brinkman-Rice transition.

For $U/t = 8$ we can deduce from Fig. 10 that the scattering amplitude for d-wave scattering from the coupling to B_{1g} modes is reduced by $\sim 60\%$ for $\delta = 0$, $\sim 50\%$ for $\delta = 0.1$, and 40% for $\delta = 0.2$ which should be compared with the 20% increase when the plasmon frequency is increased to $\Omega_{pl} = 500meV$.²⁶ Thus even the inclusion of (moderate) correlation effects leaves a significant contribution of phonons to d-wave superconductivity.

In case of the Hubbard-Holstein model¹⁸ the electron-phonon vertex is determined by the local charge response function and it turned out that the TDGA computation of this quantity is in rather good agreement with exact diagonalization and Quantum Monte Carlo results. Since for the present case of a transitive coupling detailed computations from more sophisticated approaches are not yet available a detailed comparison concerning the performance of the TDGA is not possible. However, at least our previous investigations of charge excitations on finite Hubbard clusters,^{34,35} also including the optical conductivity as an 'intersite' response function, suggest that the TDGA is a reliable approach also for the issue investigated in the present paper.

Our present study may also have relevance for an understanding of the iron-based superconductors LiFeAs and NaFeAs which, contrary to the other pnictide compounds, don't show magnetic order and have relatively low T_c ^{39,40} which suggest that an electron-phonon mechanism may play an important role. On the other hand, density functional theory results⁴¹ in coupling parameters which are far too small in order to account for the observed transition temperature. Recently, angle-resolved photoemission studies⁴² have revealed both, signatures of optical phonons and a significant electron-electron scattering rate in the spectra. One of the low energy phonon modes in the pnictides is an iron-arsenide bond-stretching phonon which affects the hopping between adjacent iron d-states in a manner similar as the

one analyzed here for the buckling modes. Thus a natural perspective of the present approach would be its combination with LDA computations for multiband Hubbard models in order to obtain a realistic estimate of correlation effects for the various phonon modes regarding their relevance for the SC pairing in low T_c pnictides.

Acknowledgments

G.S. acknowledges financial support from the Deutsche Forschungsgemeinschaft. J.L.'s research is partially supported by the Italian Institute of Technology-Seed project NEWDFESCM. M.G. and J.L. acknowledge partial financial support from MIUR-PRIN 2007 (prot. 2007FW3MJX_003).

Appendix

The elements of the interaction kernel Eq. (5) read as

$$A_{\mathbf{q}} = V_{\mathbf{q}} - \frac{L_{\mathbf{q}}^2}{U_{\mathbf{q}}} \quad (26)$$

$$B_{\mathbf{q}} = \frac{1}{2}z_0(z' + z'_{+-}) - z_0z'_D \frac{L_{\mathbf{q}}}{U_{\mathbf{q}}} \quad (27)$$

$$C_{\mathbf{q}} = - \frac{(z_0z'_D)^2}{U_{\mathbf{q}}} \quad (28)$$

with

$$\begin{aligned} V_{\mathbf{q}} &= \frac{e^0 z_0}{2} (z''_{++} + 2z''_{+-} + z''_{--}) \\ &\quad + \frac{(z' + z'_{+-})^2}{2N} \sum_{\mathbf{k}\sigma} \epsilon_{\mathbf{k}+\mathbf{q},\sigma}^0 n_{\mathbf{k}\sigma} \\ L_{\mathbf{q}} &= e^0 z_0 (z''_{+D} + z''_{-D}) + \frac{z'_D (z' + z'_{+-})}{N} \sum_{\mathbf{k}\sigma} \epsilon_{\mathbf{k}+\mathbf{q},\sigma}^0 n_{\mathbf{k}\sigma} \\ U_{\mathbf{q}} &= 2e^0 z_0 z'_D + \frac{2(z'_D)^2}{N} \sum_{\mathbf{k}\sigma} \epsilon_{\mathbf{k}+\mathbf{q},\sigma}^0 n_{\mathbf{k}\sigma}. \end{aligned}$$

Here we have defined the following abbreviations and derivatives of the hopping factors

$$\begin{aligned} z_{i\sigma} &\equiv z_0, \quad \frac{\partial z_{i\sigma}}{\partial \rho_{ii\sigma}} \equiv z', \\ \frac{\partial z_{i\sigma}}{\partial \rho_{ii-\sigma}} &\equiv z'_{+-}, \quad \frac{\partial z_{i\sigma}}{\partial D_i} \equiv z'_D \\ \frac{\partial^2 z_{i\sigma}}{\partial \rho_{ii\sigma}^2} &\equiv z''_{++}, \quad \frac{\partial^2 z_{i\sigma}}{\partial \rho_{ii\sigma} \partial \rho_{ii-\sigma}} \equiv z''_{+-}, \quad \frac{\partial^2 z_{i\sigma}}{\partial \rho_{ii-\sigma}^2} \equiv z''_{--} \\ \frac{\partial^2 z_{i\sigma}}{\partial D_i^2} &\equiv z''_D, \quad \frac{\partial^2 z_{i\sigma}}{\partial \rho_{ii\sigma} \partial D_i} \equiv z''_{+D}, \quad \frac{\partial^2 z_{i\sigma}}{\partial \rho_{ii-\sigma} \partial D_i} \equiv z''_{-D} \end{aligned}$$

Notice that in Ref. 18 the element B_q is incorrect by a factor of 'two'. Eq. (27) reports the correct expression.

-
- ¹ J. G. Bednorz and K. A. Müller, *Z. Phys. B* **64**, 189 (1986).
² J. Lee *et al.*, *Nature* **442**, 546 (2006).
³ C. Frank, in *Physical Properties of High-Temperature Superconductors IV*, edited by D. M. Ginsberg (World Scientific, Singapore, 1993), p. 189.
⁴ R. J. McQueeney, Y. Petrov, T. Egami, M. Yethiraj, G. Shirane, and Y. Endoh, *Phys. Rev. Lett.* **82**, 628 (1999).
⁵ L. Pintchovius and M. Braden, *Phys. Rev. B* **60**, R15039 (1999).
⁶ W. Reichardt, *J. Low Temp. Phys.* **105**, 807 (1996).
⁷ D. Reznik, L. Pintchovius, M. Ito, S. Iikubo, M. Sato, H. Goka, M. Fujita, K. Yamada, G. D. Gu, and J. M. Tranquada, *Nature* **440**, 1170 (2006).
⁸ B. Büchner, M. Breuer, A. Freimuth, and A. P. Kampf, *Phys. Rev. Lett.* **73**, 1841 (1994).
⁹ A. Lanzara *et al.*, *Nature* **412**, 510 (2001).
¹⁰ H. Iwasawa, J. F. Douglas, K. Sato, T. Masui, Y. Yoshida, Z. Sun, H. Eisaki, H. Bando, A. Ino, M. Arita, K. Shimada, H. Namatame, M. Taniguchi, S. Tajima, S. Uchida, T. Saitoh, D. S. Dessau, and Y. Aiura, *Phys. Rev. Lett.* **101**, 157005 (2008).
¹¹ D. R. Garcia and A. Lanzara, *Advances in Cond. Matt. Phys.* **2010**, Article ID 807412 (2010).
¹² S. Y. Savrasov and O. K. Anderson, *Phys. Rev. Lett.* **77**, 4430 (1996).
¹³ O. Gunnarsson and O. Rösch, *J. Phys.:Condens. Matter* **20**, 043201 (2008).
¹⁴ M. Capone, C. Castellani, and M. Grilli, *Advances in Cond. Matt. Phys.* **2010**, Article ID 920860 (2010).
¹⁵ Miodrag L. Kulić and Roland Zeyher, *Phys. Rev. B* **94**, 4395 (1993).
¹⁶ E. Koch and R. Zeyher, *Phys. Rev. B* **70**, 09410 (2004).
¹⁷ M. Mierzejewski, J. Zieliński and P. Entel, *Phys. Rev. B* **60**, 10442 (1999).
¹⁸ A. Di Ciolo, J. Lorenzana, M. Grilli, and G. Seibold, *Phys. Rev. B* **79**, 085101 (2009).
¹⁹ M. Grilli and C. Castellani, *Phys. Rev. B* **50**, 16880 (1994).
²⁰ S. Ishihara and N. Nagaosa, *Phys. Rev. B* **69**, 144520 (2004).
²¹ Ju H. Kim and Zlatko Tešanović, *Phys. Rev. Lett.* **71**, 4218 (1993).
²² M. Mierzejewski, J. Zieliński and P. Entel, *Phys. Rev. B* **57**, 590 (1998).
²³ R. Heid, K.-P. Bohnen, R. Zeyher, and D. Manske, *Phys. Rev. Lett.* **100**, 137001 (2008).
²⁴ R. Heid, R. Zeyher, D. Manske, and K.-P. Bohnen, *Phys. Rev. B* **80**, 024507 (2009).
²⁵ P. Zhang, S. G. Louie, and M. L. Cohen, *Phys. Rev. Lett.* **98**, 067005 (2007).
²⁶ S. Johnston, F. Vernay, B. Moritz, Z.-X. Shen, N. Nagaosa, J. Zaanen, and T.P. Devereaux, arXiv:1007.3451
²⁷ E. von Oelsen, A. Di Ciolo, J. Lorenzana, G. Seibold, and

- M. Grilli, Phys. Rev. B **81**, 155116 (2010).
- ²⁸ J. Song and J. F. Annett, Phys. Rev. B **51**, 3840 (1995).
- ²⁹ T.P. Devereaux, T. Cuk and Z.-X. Shen, and N. Nagaosa, Phys. Rev. Lett. **93**, 117004 (2004).
- ³⁰ The coupling to the local energy corresponds to a Holstein-type interaction which in connection with the Hubbard model has been discussed in Ref. 18.
- ³¹ A. Nazarenko and E. Dagotto, Phys. Rev. B **53**, R2987, (1996).
- ³² B. Normand, H. Kohno, and H. Fukuyama, Phys. Rev. B **53**, 856 (1996).
- ³³ W. F. Brinkman and T. M. Rice, Phys. Rev. B **2**, 4302 (1970).
- ³⁴ G. Seibold and J. Lorenzana, Phys. Rev. Lett. **86**, 2605 (2001).
- ³⁵ G. Seibold, F. Becca, and J. Lorenzana, Phys. Rev. B **67**, 085108 (2003).
- ³⁶ A. Comanac, L. de'Medici, M. Capone, and A. Millis, Nature Phys. **4**, 287 (2008).
- ³⁷ G. Seibold and J. Lorenzana, Phys. Rev. Lett. **94**, 107006 (2005).
- ³⁸ G. Seibold and J. Lorenzana, Phys. Rev. B **73**, 144515 (2006).
- ³⁹ Joshua H. Tapp, Zhongjia Tang, Bing Lv, Kalyan Sasmal, Bernd Lorenz, Paul C. W. Chu, and Arnold M. Guloy, Phys. Rev. B **78**, 060505 (2008).
- ⁴⁰ Dinah R. Parker, Michael J. Pitcher, Peter J. Baker, Isabel Franke, Tom Lancaster, Stephen J. Blundell and Simon J. Clarke, Chem. Commun., 2189 (2009).
- ⁴¹ R. A. Jishi and H.M. Alyahyaei, Advances in Condensed Matter Physics **2010**, 804343 (2010).
- ⁴² A. A. Kordyuk, V. B. Zabolotnyy, D. V. Evtushinsky, T. K. Kim, I. V. Morozov, M. L. Kubic, R. Follath, G. Behr, B. Buechner, S. V. Borisenko, arXiv:1002.3149.
- ⁴³ M.C. Gutzwiller, Phys. Rev. **137**, A 1726 (1965).
- ⁴⁴ G. Kotliar and A. E. Ruckenstein, Phys. Rev. Lett. **57**, 1362 (1986).
- ⁴⁵ F. Gebhard, Phys. Rev. B **41**, 9452 (1990).
- ⁴⁶ D. Vollhardt, Rev. Mod. Phys. **56**, 99 (1984).
- ⁴⁷ C. Castellani, C. Di Castro, and M. Grilli, Phys. Rev. Lett. **75**, 4650 (1995).